CORNELL ERL TOLERANCE SIMULATIONS

C. E. Mayes*, CLASSE, Cornell University, Ithaca NY 14853 USA

Abstract

Cornell University is planning to build an Energy Recovery Linac (ERL) hard x-ray lightsource operating at 5 GeV. Simulations of its approximately 3 km of electron beamline that incorporate a host of reasonable alignment and field errors, and their compensation by an orbit correction scheme, are presented. These simulations start with realistic particle distributions just after injection and track them through acceleration, the production of undulator radiation, deceleration (energy recovery), and finally transport to the beam stop. To this realistic model, single error sources are further added with increasing magnitudes in order to establish alignment and field tolerance estimates.

OVERVIEW

As for any accelerator, the Cornell ERL lattice (described in detail in [1]) is first designed while only considering linear effects. A second step refines this lattice by additionally considering collective, stochastic, and higher order effects of space-charge, coherent and incoherent synchrotron radiation, and nonlinear fields. Unfortunately, even if a computer model contains all of the correct physics, it cannot fully represent a realistic machine unless construction errors are taken into account, many of which cannot be known *ab initio*. Therefore, a third refinement of the lattice introduces random errors throughout its thousands of elements, with sizes normally distributed with specified standard deviations. Particles injected into this more realistic model should still be kept near the design orbit, and to that end a set of beam position monitors (BPMs) and orbit corrector coils are installed in the lattice.

ORBIT CORRECTION & TOLERANCES

An orbit correction scheme based on singular value decomposition (SVD) has been implemented in the Bmad and Tao accelerator simulation environments [2]. This scheme minimizes the deviation of the orbit from the design reference, with monitors located at critical locations (such as undulators and collimators) receiving extra emphasis. Additionally, the strengths of the corrector coils are added to this minimization algorithm, so that unreasonably strong fields are avoided. Finally, the dispersion is corrected at critical locations.

The placements of all monitors and correctors have been optimized using SVD decomposition techniques based on generalized error and orbit response matrices [3, 4]. This resulted in the approximately 340 BPMs and 260 corrector pairs distributed throughout the lattice.

Table 1: Tolerance Analysis Procedure. Typically this procedure is iterated for $N = 100$ times, and 4,000 Gaussian distributed macro-particles are tracked for each configuration.

Step	Procedure
1	Initialize design lattice
2	Calculate orbit and dispersion response matrices
3	Enable synchrotron radiation losses and fluctuations
4	Perturb the lattice with all of the baseline errors listed in Tab. 2
5	Additionally perturb the property to be analyzed
6	Apply the SVD orbit and dispersion correction algorithm
7	Save this perturbed lattice
8	Track particles through, and save particle statistics
9	Reset the lattice
10	Repeat steps 4-9 N times

To analyze the tolerances of various error sources, we use the procedure in Tab. 1, which leads to the allowable errors in Tab. 2. The baseline values listed in Tab. 2 represent what we currently estimate to be achievable in alignment and field quality of elements in the machine. The allowable errors are determined by limiting the increase of the projected emittance or beam size to 10% of the baseline values, or allowing 20% of the correctors to have more than 0.5 mrad maximum angles (but always less than 1.5 mrad). Note that this judgement is based on the statistics of the N runs at one standard deviation.

For example, according to Tab. 2 we find that *in addition to all of the baseline errors*, if we further misalign all quadrupole horizontal positions by 300 μm, then the horizontal corrector strengths C_x needed to correct such errors is unacceptably large. Because the baseline quadrupole horizontal offset was already 120 μm, this means that this unacceptably misaligned machine actually has rms quadrupole offsets of about $\sqrt{120^2 + 300^2}\,\mu\text{m} \approx 323\,\mu\text{m}$. Table 2 therefore shows that some errors, such as dipole pitch angles, are allowed to be much worse than the baseline value, whereas errors in cavity pitch angles should not be much worse than the baseline value.

FULL SIMULATION

The Cornell ERL has three standard operating configurations, called modes A, B, and C. Mode A operates at

* christopher.mayes@cornell.edu

Table 2: Errors Considered in Cornell ERL Simulations for the Lower Emittance Mode B (see Tab. 3). Baseline numbers are rms values with a cutoff at 3 times his value. Using only the baseline errors, the orbit at all undulators can always be corrected to the BPM resolution, which is 0.3 μm in the simulations. The symbols C_x and C_y denote horizontal and vertical corrector strengths, respectively. The symbol + indicates the maximum rms error simulated, without significant effect. OC indicates the failure of the orbit correction algorithm.

Error	Unit	Baseline (1σ)	Allowable (1σ)	Limiting Effect
Quadrupole x offset	μm	120	300	C_x
Quadrupole y offset	μm	100	250	C_y & OC
Sextupole x offset	μm	120	300	σ_y
Sextupole y offset	μm	100	200	ϵ_y & σ_y
Cryomodule quad x & y offset	μm	300	1600	C_x & C_y
Dipole roll	μrad	80	1000	ϵ_y
Quadrupole roll	μrad	80	200	ϵ_y
Dipole x & y pitch	μrad	80	5000+	ϵ_y
Quadrupole x & y pitch	μrad	80	1000+	ϵ_y
Acc cavity x & y offsets	μm	500	2000	σ_y & OC
Acc cavity x & y pitch	μrad	1000	1500	ϵ_x & ϵ_y & OC
Acc cavity gradient	relative	10^{-4}	60×10^{-4}	σ_y
Acc cavity $\phi_{\rm rf}$	degree	0.1	1.0+	σ_y
Dipole chain field	relative	10^{-4}	10×10^{-4}+	
Quadrupole k_1	relative	10^{-4}	5×10^{-4}	σ_y
Sextupole k_2	relative	10^{-4}	10^{-3}+	

100 mA, mode B operates with lower emittance and current, and mode C operates with compressed bunch lengths at lower current. These are listed in Tab. 3.

Table 2 is valid for operating modes A and B listed in Tab. 3. The 'short pulse' mode C remains to be analyzed, and will likely tighten some of the allowable errors listed here, such as the accelerating cavity phase $\phi_{\rm rf}$.

To perform full simulations for the ERL, we begin with 200,000 particles that have been tracked through optimized injector lattices, without errors, using the space-charge code GPT [5], and up through the first cryomodule in the main Linac to approximately 92 MeV. This is done for each of the operating modes in Tab. 3.

For modes A and B, particles are then tracked through the remainder of the machine with Bmad using a misaligned (and orbit and dispersion corrected) lattice, according to the baseline errors in Tab. 2. Particles for mode C are tracked using an unperturbed lattice, because the full error analysis for this mode is not yet complete. This tracking in-

Table 3: Bunch properties in the center of representative undulators, for three Cornell ERL operating modes all operating at 1.3 GHz.

Bunch Property	Mode A	Mode B	Mode C	Unit
charge	77	19	19	pC
$\gamma\,\epsilon_x$	0.31	0.13	0.66	μm
$\gamma\,\epsilon_y$	0.25	0.10	0.14	μm
σ_t	2.1	1.5	0.1	ps
σ_δ	1.66	0.66	9.3	10^{-4}

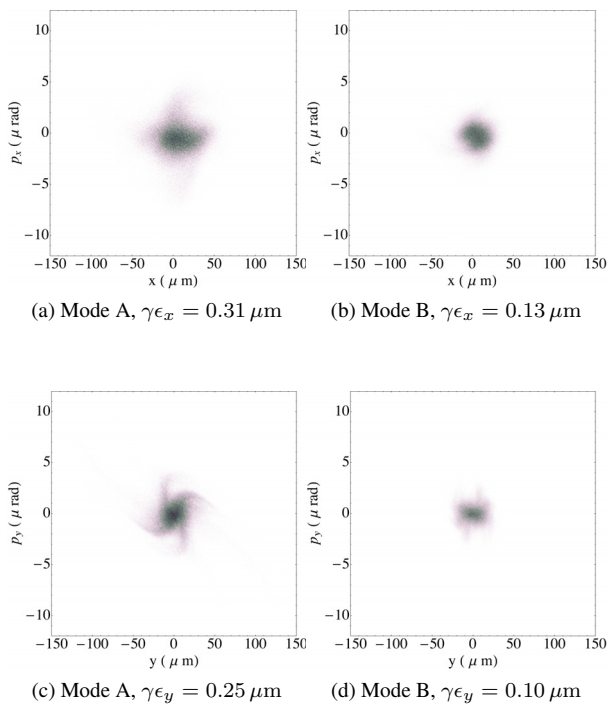

(a) Mode A, $\gamma\epsilon_x = 0.31\,\mu$m (b) Mode B, $\gamma\epsilon_x = 0.13\,\mu$m

(c) Mode A, $\gamma\epsilon_y = 0.25\,\mu$m (d) Mode B, $\gamma\epsilon_y = 0.10\,\mu$m

Figure 2: Transverse phase-space distributions at the center of undulator 1 for modes A and B in Tab. 3. These plots are are the result of splicing the 200,000 macro-particle output of GPT [5] with a misaligned and orbit corrected Bmad [2] lattices. Note that the peculiar 'tails' in Fig. 2c are preserved from the injected bunch.

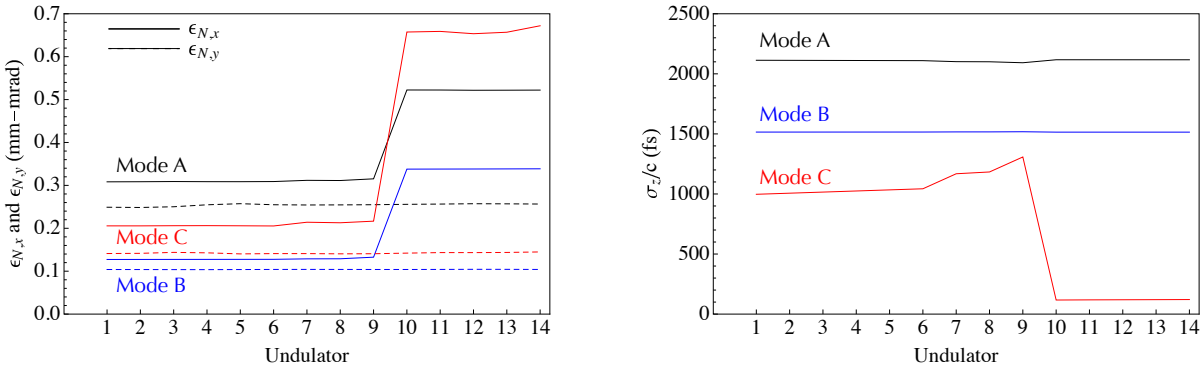

(a) Normalized Emittances

(b) Bunch Durations

Figure 1: Emittances and bunch durations for all of the ERL operating modes. Particle distributions from the output of GPT [5] are tracked using Bmad [2] through a lattice that has been misaligned (and orbit and dispersion corrected) according to the baseline errors in Tab. 2.

cludes acceleration to 5 GeV and subsequent deceleration (energy recovery) to 10 MeV. The resulting emittance and bunch durations from one particular error configuration at all 14 undulators in the machine (all at 5 GeV and numbered in order) are shown in Fig. 1.

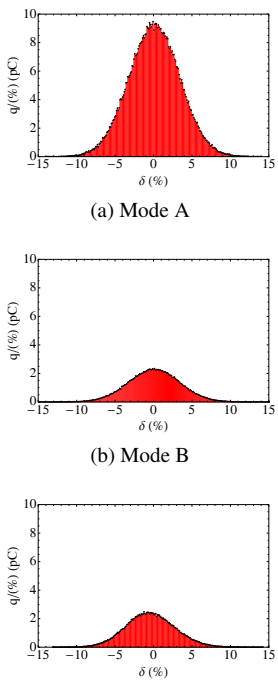

(a) Mode A

(b) Mode B

(c) Mode C

Figure 3: Final relative energy distributions just prior to the beam stop. The reference energy is 10 MeV. The standard deviation of δ for all modes is approximately 3%.

In particular, Fig. 1a shows that the emittance growth is well controlled everywhere except for a jump between undulators 9 and 10. This is almost completely due to incoherent synchrotron radiation emission in a large arc in the machine. The vertical emittance is well-preserved in all modes. The numbers in Tab. 2 are calculated at undulator 1 for modes A and B, and at undulator 10 for mode C.

For modes A and B, the usage of the more 'realistic' bunches from GPT incur no additional effects over the more simple Gaussian bunches used in the orbit correction and tolerance simulations. The compressed bunch duration of mode C particles in Fig. 1b is approximately 120 fs, but this likely can be shortened to 100 fs by minor changes in the time of flight term r_{56} and/or the accelerating phase (presently 6.6°) used in the compression scheme. Figure 2 shows the transverse phase space at the center of the first undulator for the emittance sensitive modes A and B.

Finally, we must check that these particles have an acceptable energy spread after deceleration, just prior to the demerger before the beam stop. Figure 3 shows distributions of the energy deviation δ for all three modes, all of which have an rms energy spread of $\sigma_\delta \approx 3\%$. All particles simulated lie completely within $\delta = \pm 15\%$. Note that these distributions will likely widen with the inclusion of additional wakefields, such as resistive wall and vacuum chamber roughness.

ACKNOWLEDGEMENTS

The author thanks Ivan Bazarov for providing optimized ERL injector models, as well as Georg Hoffstaetter, Florian Loehl, David Rice, and David Sagan for useful discussions. This work was supported by NSF award DMR-0807731.

REFERENCES

[1] Hoffstaetter, G. H., S. Gruner, & M. Tigner, *eds.*, Cornell ERL Project Definition Design Report (2011) `erl.chess.cornell.edu/PDDR`

[2] D. Sagan, Nuc. Instrum. Methods Phys. Res. A, **558** (2006), `www.lepp.cornell.edu/~dcs/bmad/`

[3] Ballado, A., Cornell LEPP REU Report (2010)

[4] Chao, Y.-C. & V. Mertens, LHC Project Report 470 (2001)

[5] van der Geer, S. B. & M. J. de Loos, GPT 2.8 `www.pulsar.nl/gpt`